Convergence Characteristics of a Vortex-Lattice Method for Nonlinear Configuration Aerodynamics

Z. Rusak*
Technion—Israel Institute of Technology, Haifa, Israel
A. Seginer†
NASA Ames Research Center, Moffett Field, California
and
E. Wasserstrom‡
Technion—Israel Institute of Technology, Haifa, Israel

The convergence characteristics of a vortex-lattice method for the high-angle-of-attack, nonlinear aerodynamics of aircraft and missile configurations are studied parametrically. The solution for the vortex intensities is determined by the tangency boundary condition on all of the configuration surfaces, including the three-dimensional, rolled-up wakes that characterize such flowfields. The a priori unknown position of the wake that renders this problem nonlinear is determined by an iterative process. Since there is no proof for the existence and uniqueness of this process, this paper investigates the effects of several geometrical and numerical parameters on the converged solution. It was found that the convergence of the iterative solution procedure is usually rapid and is not affected by initial conditions of the first iteration and by the integration method of the wake streamlines. Grid refinement leads to a converged solution, but its final values vary with wing surface paneling and wake discretization schemes within some range in the vicinity of the experimental data.

Nomenclature

$\mathcal{R}$ = aspect ratio
a_{ki}, b_{kj}, c_k = influence coefficients defined in Eq. (4)
b = wing span
C_{D_i} = induced-drag coefficient, $=D_i/qS$
C_L = lift coefficient, $=L/qS$
C_M = pitching-moment coefficient, $=M/qSc_{ma}$
C_{NOR} = normal-force coefficient, $=NOR/qS$
C_p = pressure coefficient, $=(p-p_\infty)/q$
ΔC_p = local load coefficient on the wing
$\bar{c}$ = mean chord, $=S/b$
c_{ma} = mean aerodynamic chord
c_r = root chord
c_v = chord of a vortex panel (Fig. 1)
D_i = induced drag
$\bar{F}$ = vector of singularity intensities, Eq. (5)
f = general function, Eq. (6)
L = lift
ℓ_w = length of rolled-up wake
M = pitching moment
NOR = normal force
N_s = number of source panels on the body
N_v = number of vortex panels on the wings
$\bar{n}$ = unit vector normal to the surface, pointing into the flow
n_c = chordwise number of vortex panels along root chord
p = static pressure
q = freestream dynamic pressure
q_i = strength of source panel number i
R = underrelaxation coefficient, Eq. (6)
S = wing area (wetted surface)
u, v, w = perturbation-velocity components
$\bar{V}_\infty$ = freestream velocity vector
$\bar{V}_n$ = vector of the freestream velocity components that are normal to the panels
x, y, z = Cartesian coordinates in the downstream, right-wing, and upward directions, respectively, measured from the wing apex
$x_{c.p.}$ = location of center of pressure
$\Delta x_w, \Delta x_p$ = length scales in the wake and on the wing panels, respectively
α = angle of attack
Γ_j = strength of bound vortex number j
μ = free-vortex shedding angle
ϕ = perturbation-velocity potential
ω = weighting parameter in second-order integration, Eq. (6)

Presented as Paper 83-1882 at the AIAA 6th Computational Fluid Dynamics Conference, Danvers, MA, July 13-15, 1983; received Aug. 2, 1983; revision received June 6, 1985.

*Graduate Student, Department of Aeronautical Engineering.
†Senior Research Associate, National Research Council. Presently, Associate Professor, Department of Aeronautical Engineering, Technion—Israel Institute of Technology, Haifa, Israel. Member AIAA.
‡Associate Professor, Department of Aeronautical Engineering. Member AIAA.

Introduction

VORTEX-lattice methods (VLM) have been widely used to compute the aerodynamic characteristics of flight-vehicle configurations (e.g., Refs. 1 and 2). The VLM is basically one of many panel methods that are described more accurately as surface-singularity methods. In general, these methods distribute panels of singularities (sources, doublets, or vortices) on the body surfaces immersed in a flow. The strengths of the singular elements are determined by satisfying the tangency boundary condition on the body surfaces. Once these are known, the influence of the body on any point in the flowfield can be computed.

Hunt[3] shows that as long as compatible boundary conditions are used, a unique solution exists for the singularity distribution. This can be proven, however, only for the so-called "linear" case, when the geometry of the wake generated by a doublet or vorticity distribution is known ab initio.[3] In practical cases the real wake is distorted after being shed and rolls up about its streamwise edges. Its geometry is part of the unknown flowfield. Since the wake is part of the boundary of the solution domain its unknown position renders the problem mathematically nonlinear.

The VLMs developed during the last decade to compute the nonlinear high-angle-of-attack aerodynamics of slender wings,[4-12] slender bodies,[13] and multi-wing-body configurations[14-17] were, therefore, composed of complicated iterative techniques that "relax" the wake to its rolled-up, force-free shape and account for the two-way interaction of the lifting surfaces with their wakes by correcting the singularity distribution with every new wake shape. Each step of the nonlinear iterative process in these methods is, in itself, a linear solution, and, therefore, has a unique solution. However, there is, no proof of the existence of a unique solution for the nonlinear procedure, even when the iterative solution converges. This lack of proof of uniqueness motivated the present authors to conduct a careful study of the convergence characteristics of their VLM for wing-body configurations.[15-17] This paper describes the method briefly and presents its convergence characteristics and sensitivity to various geometrical and numerical parameters.

Mathematical Model

Assuming a steady, incompressible, inviscid, and irrotational flow (except for discrete vortices), the disturbance-velocity potential field of a vehicle flying in a uniform flow can be described by the Laplace equation

$$\Delta^2\phi = 0 \tag{1}$$

If the flow is subsonic and small perturbations are assumed, the following discussion will also apply when the Prandtl-Glauert equation is substituted for Eq. (1).

The solution to the Laplace equation is determined by the tangency boundary condition

$$\frac{\partial\phi}{\partial\bar{n}} + \bar{V}_\infty \cdot \bar{n} = 0 \tag{2}$$

that has to be satisfied everywhere on the configuration surfaces, and by the requirement that the perturbations vanish at infinite distances from the configuration. The vortical wakes shed by the lifting surfaces cannot support a pressure difference and, therefore, have to be free-vortex sheets locally tangent to the stream surface. The tangency condition of the wake to the stream surface implies satisfaction of Eq. (2) on the wake as well. This makes the wake portion of the computational-domain boundary,[3] and its unknown location, to be found iteratively, makes the problem nonlinear, although the Laplace equation is linear.

Green's third identity reduces the problem of finding the volume distribution of a potential function to the problem of finding a surface distribution of singular elements (sources or doublets) that satisfies the boundary conditions. In the present method, the body alone is assumed to be nonlifting and is modeled by a distribution of source panels only. The lifting surfaces are assumed to be of zero thickness and are modeled by a vortex lattice (equivalent to a piecewise-constant doublet distribution[3]). The trailing parts of the bound vortices that simulate the vorticity shed by the lifting surfaces are free-vortex lines. The continuity in pressure across the wake is imposed by making the vortex lines coincide with the streamlines,

$$\frac{dy}{dx} = \frac{v}{V_\infty + u}; \quad \frac{dz}{dx} = \frac{w}{V_\infty + u} \tag{3}$$

from the shedding point into the far wake. Satisfying Eq. (3) along all of the wing edges (leading, side, and trailing edges) also satisfies the Kutta condition, but from the wake direction only.

Method of Solution

The body is simulated by a conventional source-panel method.[18] The body is approximated by a number (N_s) of trapezoidal panels carrying a piecewise-constant source distribution of unknown strength q_i. The collocation point at which the boundary condition [Eq. (2)] is satisfied is at the center of the panel area. A typical paneling scheme of the body is shown in Fig. 1.

The flowfield generated by the lifting surfaces is described by a nonlinear VLM.[11] The zero-thickness lifting surfaces are divided into a number (N_v) of vortex panels that are mostly rectangular. However, the triangular panels of Rom et al.[8] are used along the edges of swept wings (Fig. 1). A discrete horseshoe vortex of unknown strength Γ_j is bound to the ¼-chord line of each panel. The trailing arms of the vortex also are bound to the surface along the panel streamwise demarcation lines until they reach one of the wing edges. From there they are shed as free vortices. The collocation points on the vortex panels are located at the intersection of the longitudinal median of the panel with its ¾-chord line.

With body and wing paneling defined, there remains the question of the wing-body junction and the lift carryover from the wing to the body. References 15 and 19 discuss the necessity to continue the vorticity distribution of the wing either on the body surface or through the body. In the present method, the bound vortices adjacent to the body are extended into the body up to the plane of symmetry, thus eliminating the strong trailing vortex that otherwise would be generated at the wing-body juncture. The extended vortices have no collocation points of their own, but their induced velocities are accounted for in the satisfication of the boundary conditions on all surfaces and wakes.

An initial guess of the shape of the wake is needed to start the solution process. The trajectories of the free vortices are usually assumed to be semi-infinite straight lines, leaving the wing edges at some predetermined angle μ below the freestream direction.

To find a solution one has only to satisfy the tangency boundary condition [Eq. (2)] simultaneously at all of the collocation points. This results in a system of $(N_s + N_v)$ linear algebraic equations for the unknown intensities of the sources and vortices

$$\sum_{i=1}^{N_s} a_{ki} q_i + \sum_{j=1}^{N_v} b_{kj} \Gamma_j + c_k = 0 \quad (k = 1,2,\ldots,N_s + N_v) \tag{4}$$

where $c_k = (\bar{V}_\infty \cdot \bar{n})_k$ is the component of the freestream velocity normal to the panel number k at its collocation point, and a_{ki} and b_{kj} are the influence coefficients of the source panel i and the vortex j, respectively, on the collocation point of panel k. An influence coefficient is defined as the normal component $(\partial\phi/\partial\bar{n})_k$ of the velocity that is induced on panel k by a singular potential element of unit strength. The influence of a vortex includes the influence of its trailing free arms, requiring the predetermination of their spatial location. Detailed formulas for the influence coefficients are given in Ref. 15.

Rewritten in matrix form, Eq. (4) becomes

$$[BW]\bar{F} + \bar{V}_n = 0 \tag{5}$$

where $[BW]$ is an (N_s+N_v) square matrix of the influence coefficients; $\bar{F}$ the vector of singularity intensities, $\bar{F}=\{\frac{q_i}{\Gamma_j}\}$; and $\bar{V}_n$ the vector $\bar{V}_n=\{c_k\}$.

Equation (5) is solved for the intensities of the singular elements (q_i, Γ_j). This is a linear problem and, in principle, has a unique solution. With these intensities known, the velocities induced by them on any point in the flowfield can be computed and Eq. (3) can be integrated for the trajectories of the free vortices. The integration is carried out up to some predetermined distance (l_w), where the free-vortex lines are replaced by semi-infinite straight lines parallel to $\bar{V}_\infty$. The vortex lines define a new wake shape that is used to recompute the singularity intensities from Eq. (5). The calculation cycle (Fig. 2) is reiterated until the wake solution converges to a constant shape.

Once the computation is converged, the load distribution on the lifting surfaces is computed from the Kutta-Joukowski theorem, and the pressure distribution on the body is obtained from the Bernoulli equation. These distributions are integrated to compute the lift, induced-drag, and pitching-moment coefficients. Details of all of the calculations are given in Ref. 15. Validation of the linear mode of the computer code is described in Ref. 17.

Parameters Influencing Convergence

In the present iterative procedure it is the changing shape of the wake that determines the solution. It is also the last feature of the flowfield to converge (the integral aerodynamic coefficients converge first, and the pressure distribution is second). Therefore, it is assumed that the wake parameters and its numerical treatment influence the convergence rate and the converged solution.

The wake parameters that may influence the convergence process, and have been studied here, are:

1) The integration method of the free-vortex trajectories [Eq. (3)].

2) The cutoff distance for the interaction of two close free vortices, or for the interaction of a free vortex with a very close vortex panel.

3) The length of the integrated rolled-up wake l_w.

4) The initial guess of the shedding angle μ of the free vortices.

These parameters were also studied to some degree in Refs. 4-14 and, therefore, will be dealt with here only briefly. More attention will be paid to two additional parameters that were only briefly mentioned:

1) The paneling scheme and its effects on the free-vortex trajectories and on the wing-body juncture problem.

2) The effects of grid refinement in the wake and on the solid surfaces.

Free-Vortex Trajectory Integration

Equation (3) can be integrated by several methods. The general second-order integration of $dy/dx=f(x,y)$ (the two-dimensional example was chosen for the sake of simplicity only) is

$$y_{i+1}=y_i+R(\Delta x)\{(1-\omega)f(x_i,y_i)+\omega f[x_i+(\Delta x/2\omega), y_i + (\Delta x/2\omega)f(x_i,y_i)]\}+\emptyset(\Delta x^3) \quad (6)$$

where R is an underrelaxation coefficient $(0<R\leq 1)$. The usual second-order integration uses $\omega=0.5$. With $\omega=0$, Eq. (6) is reduced to the simple, first-order Euler integration method, and $\omega=1$ gives an improved Euler scheme. In addition to these three methods, a second-order Runge-Kutta predictor-corrector also was used.[15]

Only small differences between the converged solutions, obtained with these methods, were found.[8,11,16] Therefore, the first-order Euler scheme is recommended, since it is the least time consuming per iteration. The convergence rate of this scheme can be accelerated when the most recently updated wake shape is used to compute the induced velocities in Eq. (3) for the next grid point. No difference was found between consecutive Euler integrations along single vortex lines out to the far wake and a simultaneous Euler integration across the wake that is marched downstream.

In conclusion, the integration method of the wake shape was found to have no effect on the convergence process of the solution.

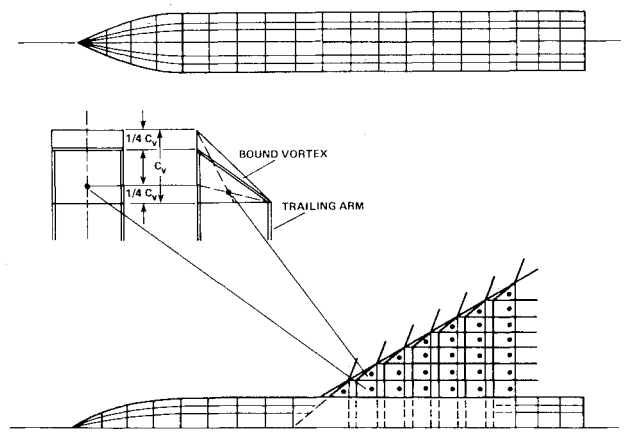

Fig. 1 Paneling scheme of a wing-body configuration.

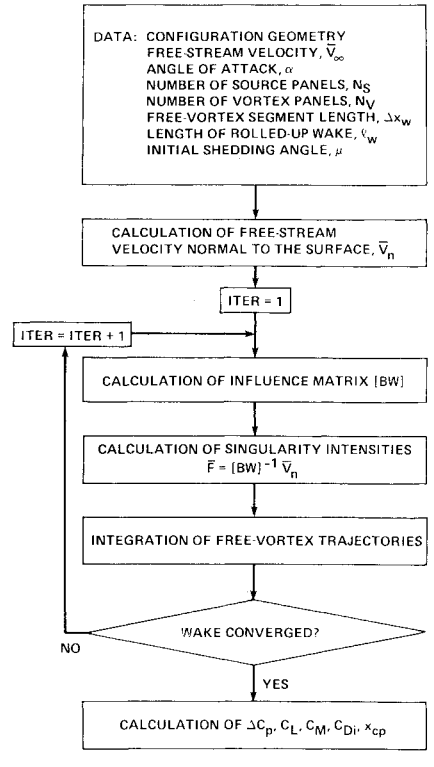

Fig. 2 Flowchart of the iterative computation procedure.

Cutoff Distances for a Strong Interaction

During the iterations for the shape of the wake a free vortex is apt to pass close to another free, or bound, vortex. The very high velocities induced at a close proximity of two potential vortices may cause the solution to diverge. This problem can be eliminated by preventing the induced velocity from increasing above a certain level. To achieve this purpose a "viscous core" (solid-body rotation)[8] or a constant induced velocity[8,16] is used below a lower bound on the distance separating two

vortices, which is often called the "cutoff distance." The specification of the cutoff distance is based on empirical considerations and has no theoretical basis or physical justification. Results of numerical experimentation[16] indicate that it should be bounded from below by one-tenth of the smaller of the surface-panel dimensions, and from above by one-quarter of the same dimension. Above the upper bound the interaction is not fully accounted for. Below the lower bound the induced velocities are too strong and the solution may diverge. The wake rollup in both cases is incorrect.

The source panels that simulate the body do not need a cutoff distance because their induced velocities are bounded by the strength of the panel singularity.[18] Furthermore, the body source panels usually induce an outward velocity on the free vortices, thus preventing them from piercing the body or even from passing too close.

Length of the Rolled Up Wake

The detailed computation of the shape of the rolled up wake is performed from the vortex shedding points to a prescribed distance (l_w). Farther downstream, in the "far wake," the vortices are continued to infinity as straight lines. This practice saves computation time, since longer rolled up wakes use more computer time and memory volume.

The effect of this prescribed distance on the computational results was small. The variations of the lift and pitching-moment coefficients of two delta wings (aspect ratios of 2.0 and 1.0 at $\alpha = 20$ deg) with l_w are shown in Fig. 3. A rolled up wake length of half the mean aerodynamic chord was sufficient for the convergence of the aerodynamic coefficients.

Initial Shedding Angle

The common initial guess of the wake shape in the first iteration cycle of the computation is a planar wake deflected down from the freestream direction at an angle μ. Angles between $\mu = 0$ deg (aligned with $\bar{V}_\infty$) and $\mu = \alpha$ (aligned with the chord) were found to have no effect on the converged aerodynamic coefficients of two delta wings,[17] but little effect on their convergence rate (Fig. 4a). The convergence was rapid even when the wake was initially deflected upward, too far away from its final position, as was done on the missile model in Fig. 4b.

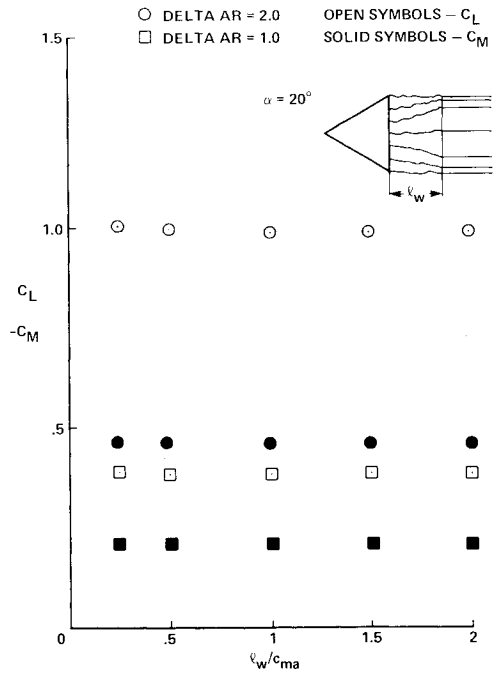

Fig. 3 Effects of rolled up wake length on the converged solution.

Effects of Paneling Scheme

Whereas the various paneling schemes (e.g., trapezoidal panels with a piecewise-constant doublet distribution,[17] classic VLM trapezoidal panels,[1-2] and rectangular-triangular VLM paneling scheme[8]) had no effect on the linear solutions,[17] this was not the case in the nonlinear problems. The simulation of the leading-edge separation on delta wings necessitated the use of triangular vortex panels along the swept leading edges. Three different paneling schemes were used: 1) Rom-Zorea scheme,[8] also used in the present work (Fig. 5a); 2) Kandil-Mook-Nayfeh scheme[9] (Fig. 5b); and c) Gordon-Rom scheme[12] (Fig. 5c). Although the integral aerodynamic coeffi-

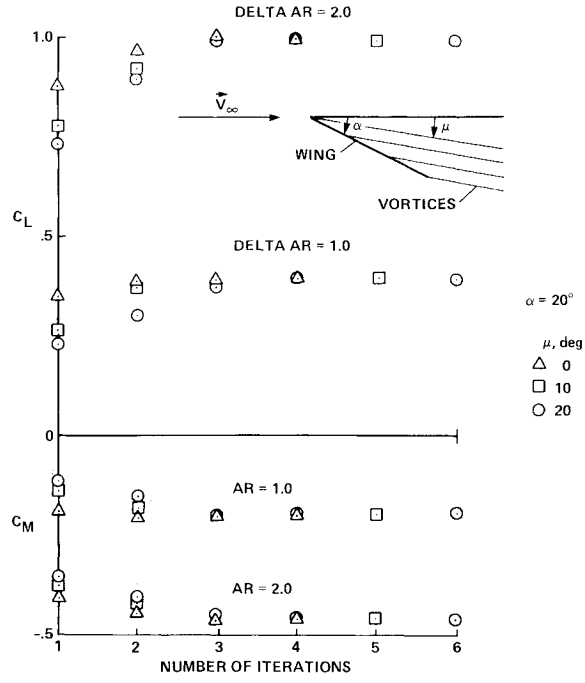

a) Shedding angles between the freestream and wing plane.

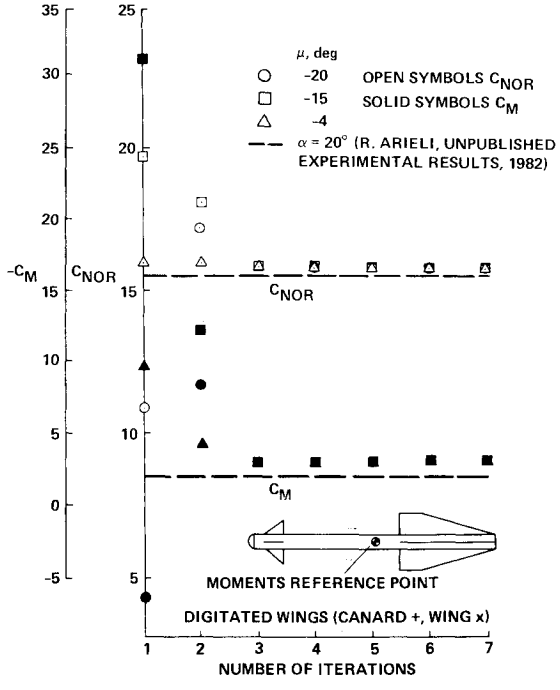

b) Wake deflected far above the wing.

Fig. 4 Effects of the initial shedding angle on convergence rate.

cients of slender configurations were predicted fairly well by all three schemes,[4-17] differences were found in the details of the flowfield.[17]

The various effects of the triangular paneling schemes on the surface pressure distributions and on the shape of the wake were demonstrated by Ref. 17 and were also discussed in Ref. 12. It was found[17] that the strengths of the vortices in the leading-edge panels depended on the paneling scheme, and had a direct effect on the pressure distribution and on the shape of the rolled up wake. It was pointed out in Ref. 17 that the differences between the schemes in Fig. 5 are in the vortex length and its distance to the collocation point. Both of these factors affect the strength of the vortex. Reference 17 suggests that maintaining a constant ratio of the length of the bound vortex to its distance to the collocation point would acheive the best results. A constant ratio has been used in Ref. 12 by substituting a standard rectangular panel for the leading-edge triangular panel, whereas this ratio varied with the aspect ratio in the schemes of Refs. 8 and 9. However, the physical meaning of extending the bound vortices rigidly into the outer flow[9,12] is unclear. In fact, the mathematical model of the delta wings of Refs. 9 and 12 resembles a wing with sawteeth, which must certainly have different aerodynamic characteristics than straight-edged delta wings.

It is interesting to note in Ref. 20 that the direction of the bound-vortex lines at the leading edge resembles that of the paneling scheme of Ref. 9 near the apex, that of Ref. 12 in the midsection, and that of Ref. 8 near the trailing edge. Apparently some mix of all three would be best.

Another pitfall to be avoided that may result from the paneling scheme concerns the wing-body juncture line. The juncture line must also be a common demarcation line of the vortex panels on the wing and of the adjacent source panels on the body. Both of these panels must also have the same streamwise dimension so that the spanwise demarcation lines on the wing merge with the circumferential lines on the body. A mismatch of the two panel distributions can cause unrealistically strong local interactions and a deviation from the correct solution even in the linear case.

Grid Refinement

In a finite difference solution of a differential equation, a mesh refinement should, in principle, converge to the solution of the differential equation itself, whereas in VLMs there is no reason that it should.[3] The tangency boundary condition is satisfied at the collocation points only, while everywhere else the fluid "leaks" through the surface. This leak will not be eliminated by grid refinement. Still, the character and trends of the variation of the solution with vortex-grid refinement are indicative of the uniqueness of the solution.

The nonlinear VLM has two supposedly independent length scales. One is the length (Δx_w) of the free-vortex segments in the wake used in the integration of the wake shape [Eq. (3)]. The other is the length (or chord) of the vortex panel ($\Delta x_p = c_r/n_c$). A reduction in Δx_w should result in a smoother vortex line that is closer to the exact solution of the streamline equations. The effect of the reduction in the vortex-segment length on the lift coefficients of two delta wings ($\mathcal{R} = 1.0$ and 2.0 at $\alpha = 20$ deg) is shown in Fig. 6 for several constant vortex-panel sizes. Also shown for comparison are the experimental lift coefficients of Ref. 21. When the length of the vortex panel (Δx_p) is kept constant, the ratio of panel length to vortex-segment length ($\Delta x_p/\Delta x_w$) goes to infinity as Δx_w goes to zero. The lift coefficient does exhibit a convergent character when the segment length is reduced. However, when Δx_w becomes much smaller than the panel length (typically less than one-quarter of Δx_p), the iteration process becomes unstable and diverges. This is probably the result of the finer representation that may induce higher curvature in the vortex lines. A highly curved vortex generates high self-induced velocities that can cause divergence of the iterative process. With very long wake segments the differences between the solutions with different segment lengths can be large (Fig. 6). This is probably the effect of a large step in the integration of Eq. (3) that can accumulate a large error.

Furthermore, Fig. 6 also shows a very strong effect of the panel size on the lift coefficient. This effect is investigated in Fig. 7, where the lift coefficients of the same two wings are plotted as a function of the total number of vortex panels on one-half of the wing (one-half was sufficient for a symmetric solution). This is done for several constant wake-segment lengths. The experimental lift coefficients also are shown for comparison. The lift coefficient increases with grid refinement and shows a tendency to approach a constant value exponentially. However, this final value depends on the length of the free-vortex segment.

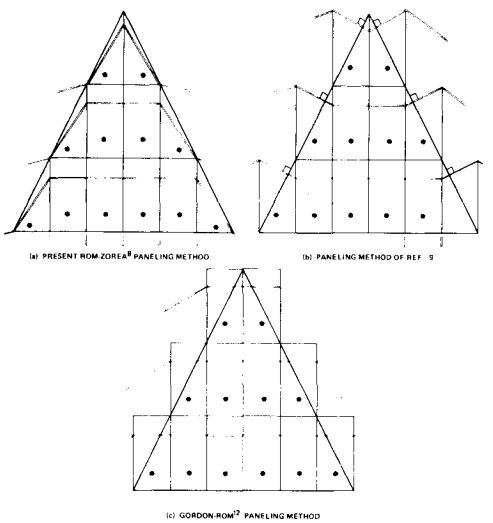

Fig. 5 Comparison of paneling methods for nonlinear aerodynamics.

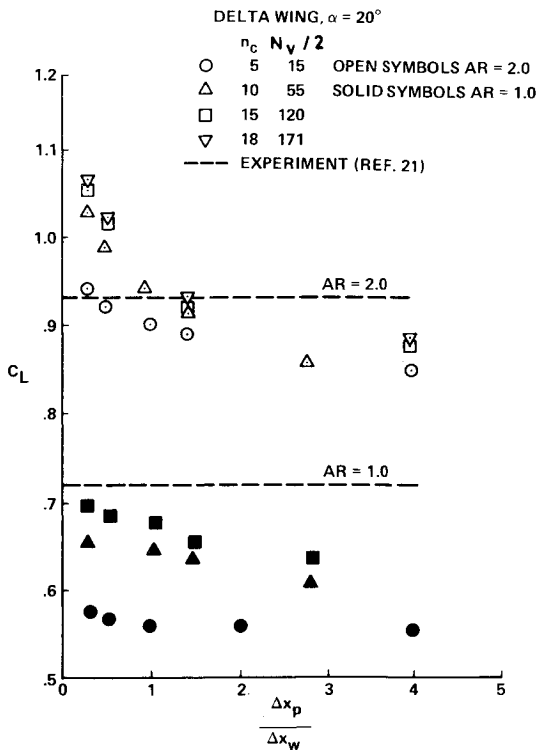

Fig. 6 Convergence of the lift coefficient with the reduction in the free-vortex segment length.

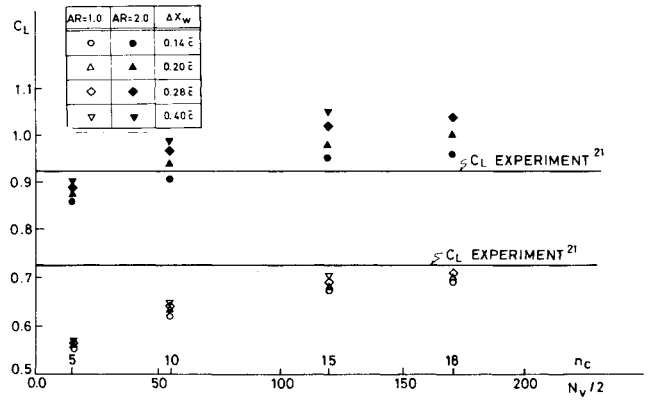

Fig. 7 Convergence of the lift coefficient with grid refinement on the wing only.

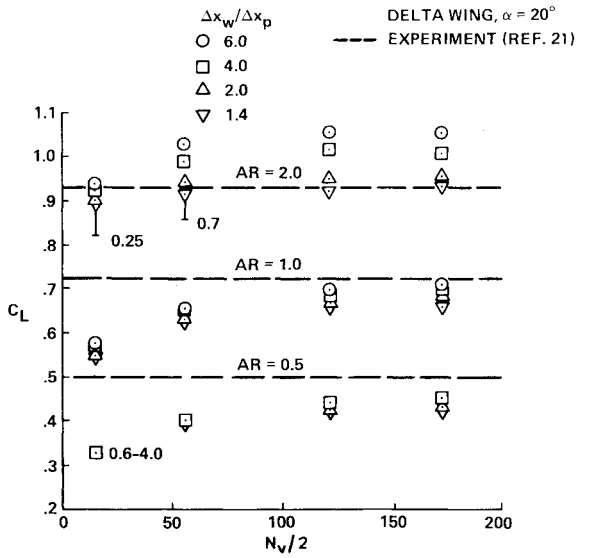

a) Lift coefficient.

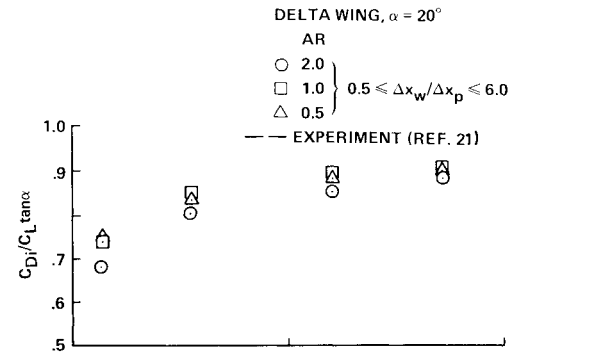

b) Induced drag.

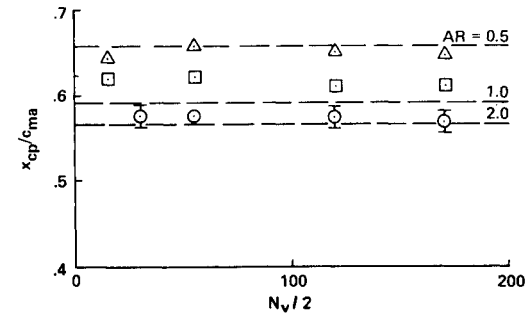

c) Center of pressure.

Fig. 8 Effects of grid refinement on the aerodynamic characteristics of the wings.

To isolate the dependence of the results on the two length scales, the previous results are replotted in Fig. 8 as the variations of the lift coefficient, the induced-drag coefficient, and the location of the center of pressure with the increasing number of vortex panels for several constant ratios of the free-vortex segment length to panel length. By using this ratio as a parameter, the grid refinement applies simultaneously to both characteristic lengths. The aerodynamic coefficients show a tendency to reach their final values at, or above, 171 vortex panels (on a half-wing). The final value of the lift coefficient depends on the wake-segment-to-panel-length ratio (Fig. 8a). A similar behavior observed by Gordon and Rom,[12] who used a different paneling scheme, indicated that this effect of the length ratio is not a result of the paneling method. It has also been shown analytically in Ref. 22, that the length-scale ratio plays a primary role in the numerical formulation of the VLM that is independent of the paneling scheme and, consequently, also has a primary influence on the results and convergence of the iterative solution process.

A comparison of the computed lift coefficients with experimental data for three delta wings (Fig. 8) offers an approximate engineering formula for the choice of a length ratio that, when used for delta wings in the present method, results in convergence with grid refinement to lift coefficients that are in fair agreement with the experimental data. For delta wings with aspect ratios from 0.5 to 2.0, a ratio of $(\Delta x_w)/(\Delta x_p) \cong 4/(\mathcal{R}^2 - \mathcal{R} + 0.6)$ is recommended, although no reasonable explanation can be offered for this correlation at this stage.

It is interesting to note that the ratio of the induced drag to the component of the normal force in the free-flow direction (which should be 1.0), $C_{D_i}/(C_L \tan\alpha)$, and the location of the center of pressure (Figs. 8b and 8c), are not dependent on the length-scale ratio. Apparently C_{D_i} varies similarly to C_L and the variation of the load distribution over the wing with both grid refinement and length-scale ratio is self-similar.

Conclusions

The convergence characteristics of the iterative vortex-lattice solution for nonlinear aerodynamics have been thoroughly investigated by numerical experimentation. It is shown herein that the iterative solution procedure usually converges. Divergence can be prevented by a proper choice of a cutoff distance for the interaction of close singularities and by an underrelaxation of the iterative correction of the wake shape. The convergence of the iterative procedure is independent of the specific integration method of the trajectories of the free vortices and of the initial guess for the vortex-shedding angle. The far-wake approximation can be applied at the relatively short distance of one-half the mean aerodynamic chord behind the wing trailing edge with no detrimental effects on the computed results.

Although grid refinement leads to convergence, the lift coefficient converges to different values, depending on the ratio of the free-vortex segment length to the panel length. An optimum length-scale ratio is recommended for engineering use.

The local details of the solution, such as the load distribution, shape of the wake, and induced cross-flow velocities, have a strong dependence on the wing paneling method and vortex model even when the integral aerodynamic coefficients converge to the same values. This would not affect users who require only the overall aerodynamic coefficients. However, users who need the local details of the flowfield should be aware of the limitations of the vortex-lattice method and should ensure that the vortex model and paneling used are adequate for their problem.

References

[1]Margason, R. J. and Lamar, J. E., "Vortex Lattice Fortran Program for Estimating Subsonic Aerodynamic Characteristics of Complex Planforms," NASA TN D-6142, Feb. 1971.

[2]"Vortex Lattice Utilization," NASA SP-405, May 1976.

[3]Hunt, B., "The Mathematical Basis and Numerical Principles of the Boundary Integral Method for Incompressible Potential Flow over 3-D Aerodynamic Configurations," *Numerical Methods in Applied Fluid Dynamics*, Academic Press, London, 1980, pp. 49-135.

[4]Hedman, S. G., "Computation of Vortex Models for Wings at High Angle of Attack in Incompressible Flow," Aeronautical Research Institute of Sweden, Bromma, Sweden, FFA AU-653, Feb. 1973.

[5]Maskew, B., "The Calculation of Potential Flow Aerodynamic Characteristics of Combined Lifting Surfaces with Relaxed Wakes," Hawker Siddeley Aviation, Kingston, U.K., Note YAD-3192, Sept. 1973.

[6]Rehbach, C. "Étude Numérique de Nappes Tourbillonnaires Issues d'Une Ligne de Decollement Près du Bord d'Attaque," *Recherche Aerospacialle*, Vol. 1973 (153), Nov.-Dec. 1973, pp. 325-330.

[7]Mook, D. T. and Maddox, S. A., "Extension of a Vortex-Lattice Method to Include the Effects of Leading-Edge Separation," *Journal of Aircraft*, Vol. 11, Feb. 1974, pp. 127-128.

[8]Rom, J., Zorea, C., and Gordon, R., "On the Calculation of Nonlinear Aerodynamic Characteristics and the Near Vortex Wake," ICAS Paper 74-27, Aug. 1974.

[9]Kandil, O. A., Mook, D. T., and Nayfeh, A. H., "Nonlinear Prediction of the Aerodynamic Loads on Lifting Surfaces," *Journal of Aircraft*, Vol. 13, Jan. 1976, pp. 22-28.

[10]Kandil, O. A., Mook, D. T., and Nayfeh, A. H., "A Numerical Technique for Computing Subsonic Flow Past Three-Dimensional Canard-Wing Configurations with Edge Separations," AIAA Paper 77-1, Jan. 1977.

[11]Rom, J., Almosnino, D., and Zorea, C., "Calculation of the Nonlinear Aerodynamic Coefficients of Wings of Various Shapes and Their Wakes, Including Canard Configurations," *Proceedings of the 11th ICAS Congress*, Vol. 1, Sept. 1978, pp. 333-344.

[12]Gordon, R. and Rom, J., "Calculation of Aerodynamic Characteristics of Wings with Thickness and Camber by a New Method Based on the Modified Vortex Lattice Method," Technion—Israel Institute of Technology, Israel, TAE Rept. 493, July 1982.

[13]Almosnino, D. and Rom, J., "Calculation of Symmetric Vortex Separation Affecting Subsonic Bodies at High Incidence," *AIAA Journal*, Vol. 21, March 1983, pp. 398-406.

[14]Atta, E. H. and Nayfeh, A. H., "Nonlinear Aerodynamics of Wing-Body Combinations," AIAA Paper 78-1206, July 1978.

[15]Rusak, Z., "Numerical Calculation of Wing-Body Configurations," M.Sc. Thesis, Technion—Israel Institute of Technology, Haifa, Israel, Jan. 1982.

[16]Rusak, Z., Wasserstrom, E., and Seginer, A., "Numerical Calculation of Nonlinear Aerodynamics of Wing-Body Configurations," *AIAA Journal*, Vol. 21, July 1983, pp. 929-936.

[17]Seginer, A., Rusak, Z., and Wasserstrom, E., "Convergence Characteristics of Nonlinear Vortex-Lattice Methods for Configuration Aerodynamics," AIAA Paper 83-1882, July 1983.

[18]Hess, J. L. and Smith, A. M. O., "Calculation of Potential Flow About Arbitrary Bodies," *Progress in Aeronautical Sciences*, Vol. 8, Pergamon Press, NY, 1967, pp. 1-138.

[19]Hess, J. L., "Calculation of Potential Flow About Arbitrary, Three-Dimensional Lifting Bodies," McDonnell Douglas Corp., St. Louis, MO, Rept. MDC J5679-01, Oct. 1972.

[20]Hummel, D., "On the Vortex Formation Over a Slender Wing at Large Angles of Incidence," AGARD CP-247, Paper 15, Oct. 1978.

[21]Wentz, W. H. Jr., "Effects of Leading-Edge Camber on Low-Speed Characteristics of Slender Delta Wings," NASA CR-2002, Oct. 1972.

[22]Rusak, Z. and Seginer, A., "An Analytical Parametric Investigation of Numerical Nonlinear Vortex-Lattice Methods," *Collection of Papers, 27th Israel Annual Conference Aviation and Astronautics*, Tel-Aviv, Israel, Feb. 1985, pp. 13-22.